PHYSICAL REVIEW B VOLUME 26, NUMBER 10 15 NOVEMBER 1982

Effects of barrier preparation on inelastic electron tunneling

R. A. Dragoset, E. S. Phillips, and R. V. Coleman
Department of Physics, University of Virginia, Charlottesville, Virginia 22901
(Received 25 January 1982; revised manuscript received 30 July 1982)

Al-AlO_x-Pb junctions prepared for inelastic-electron-tunneling spectroscopy (IETS) have been studied as a function of OH structure associated with the AlO_x barrier. The charged OH structure has been modified by cooling and roughening the substrate and by varying the exposure to H_2O during fabrication. A model barrier calculation using a WKB approximation for the tunneling current and a computer fitting procedure for obtaining a fit to the experimental *I-V* curves has allowed quantitative comparison of the barrier parameters resulting from the different preparation procedures. In all cases the AlO_x barrier asymmetry is dominated by the charged OH structure and the polarizable dipole layer associated with this interface structure. Cooling the substrate or roughening the substrate during preparation enhances the OH mode structure and reduces the barrier asymmetry by several electron volts from that observed for standard room-temperature preparation of smooth junctions. Exposure of rough substrates to water vapor can completely reverse the barrier asymmetry. The contribution of the OH groups can be modeled as a dipole layer contributing a high, thin barrier near the second electrode. A two-barrier model can be used to fit the elastic-tunneling data quite well. For doped junctions used for molecular-vibrational-mode analysis an enhanced OH structure contributed by the barrier generally produces a strong reduction of vibrational-mode intensity. A sharp, well-defined dipole layer appears to enhance the IET spectrum, possibly through the presence of a high, thin barrier as well as through the detailed polarization properties of the barrier. Additional OH adsorption reduces and disorders this barrier, leading to less electron-phonon coupling in the excitation of IETS modes.

I. INTRODUCTION

The use of inelastic-electron-tunneling spectroscopy (IETS) to study the vibrational spectra of molecules has been expanded to cover a wide range of applications[1–3] and is a particularly sensitive technique for studying molecules adsorbed at interfaces. A critical component in this technique is the formation of a suitable tunneling barrier on which the molecules to be studied are either chemisorbed or physisorbed. In the majority of the IETS applications so far reported, this barrier has been AlO_x formed on an evaporated Al film serving as one of the electrodes in the tunnel junction. The structure and surface state of this oxide can have a significant effect on the resulting IET spectra and a complete characterization of the oxide-barrier effects on IET spectra is essential for development of the IETS technique.

In this paper we report the results of experiments which modify the detailed behavior of the AlO_x barrier and analyze the effects on both the elastic- and inelastic-tunneling characteristics of the IETS junctions prepared with AlO_x barriers. Major effects on the barrier shape and height and on the inelastic-mode intensity have been observed for different preparation procedures carried out during the barrier fabrication.

AlO_x barriers formed by both thermal oxidation and plasma-discharge oxidation have been studied. The amount of H_2O present during the oxidation procedure can modify the junction behavior and has been found to depend on such factors as the temperature of the doped substrate during deposition of the top electrode and on the roughness of the barrier surface. Some of these modifications are reversible, while others are not. The detailed behavior is very sensitive to the charge structure at the barrier-electrode interface and has been correlated with the effective-barrier heights by fitting the measured *I*-vs-*V* characteristics to a WKB expression for the elastic-tunneling current.

II. EXPERIMENTAL TECHNIQUES

The Al-AlO_x-Pb junctions were fabricated in an oil-diffusion-pumped vacuum system using the following sequence of steps. Five thin-film aluminum strips ($\sim$2000-Å thick) were evaporated from a resistively heated tungsten coil onto a precleaned glass microscope slide at a vacuum of 10^{-6} Torr. The thermal-oxide barriers were formed by admitting room air at room temperature. The plasma-discharge barriers were produced by plasma discharge in $\sim$20 mTorr of O_2 at 750 V and 20 mA for 1—5 min. For undoped junctions the vacuum system was immediately repumped to 10^{-6} Torr and the overlaid Pb strip evaporated from a molybdenum boat. In the case of doped junctions the slide was transferred from the vacuum system to a laminar flow hood and doped using liquid-phase doping as initially described by Hansma and Coleman.[4] The doped AlO_x substrate was then returned to the vacuum chamber and repumped to 10^{-6} Torr followed by evaporation of the lead cross strip.

Dopant solutions were prepared beforehand using triply distilled water or ethanol as solvents. Solution concentrations varied from 0.02 to 5 mg/ml in order to adjust the coverage to give the desired junction resistance in the range 100—3000 Ω. The chemicals and solvents were to spectrograde purity and were obtained from the Aldrich, Eastman, and Calbiochem chemical companies.

For the junctions prepared using cooled substrates the glass slides and masks were mounted directly on a liquid-nitrogen-cooled copper block. The temperature of the substrate was monitored using a copper-constantan thermocouple in direct contact with the aluminum electrodes.

The rough substrates were prepared by first evaporating a thin film of CaF_2 over the microscope slide. The junction preparation was then carried out with the same sequence as described above. The CaF_2 films were more than 900-Å thick and, according to data from Endriz and Spicer[5] and Bennett *et al.*,[6] the aluminum films evaporated onto the CaF_2 films will have an atomic scale roughness of 20—40 Å. This should create an AlO_x barrier with a surface roughness on the same order as the average thickness of the barrier, which is estimated to be (10—20)-Å thick.

For junction preparation in which excess water vapor was used, the water vapor was evaporated directly into the vacuum-preparation chamber from a glass chamber containing liquid H_2O.

The I-vs-V curve obtained from the junction is a sum of the elastic- and inelastic-tunneling contributions to the current. Owing to the very small relative component of inelastic current ($\sim$1%), the measurements of interest include dV/dI vs V and d^2V/dI^2 vs V, as well as I vs V. Measurements were made by incorporating the junction into a bridge circuit developed after Adler *et al.*[7] A 500-Hz ac modulation voltage with an amplitude of 1—3 mV peak to peak was applied to the junction and the first- and second-derivative curves were then recorded directly using conventional harmonic detection with a lock-in amplifier. The resolution of the second-derivative plot, or tunneling spectrum, is on the order of 8 cm^{-1}. The I-vs-V curve was recorded by placing a resistor in series with the junction to obtain a voltage proportional to the current and by measuring the voltage applied directly to the junction. The data were all taken at 4.2 K with the Pb electrode superconducting. The IET spectra have been shifted by $\sim$8 cm^{-1} to account for the superconducting gap.

The computer fits to the I-vs-V curves were obtained using a modification of the expression given by Brinkman *et al.*[8] using the WKB approximation and assuming perfectly sharp boundaries between electrodes and insulator. The detailed barrier models and current expression are discussed in Sec. IV A. Computer programs have been developed for the CDC Cyber-176 and DEC PDP 11/34 computer systems and fits to the I-vs-V curves have been made for the range 0 to $\pm$1 V. Further details of the barrier modeling procedure can be found in the article by Korman *et al.*[9]

All intensity comparisons between IET spectra have been made using spectra recorded at the same modulation voltage and using the same sensitivity settings on the bridge electronics and lock-in amplifier. The intensity units have not been calibrated, but the same magnitude of intensity unit has been used for all spectra.

III. EXPERIMENTAL RESULTS

A. Standard AlO_x barriers

IETS junctions prepared in high-purity vacuum systems without doping show inelastic-vibrational-mode structure arising from the oxide. In both the thermal- and plasma-discharge oxides prepared at room temperature under normal vacuum conditions, the most prominent mode is an intense broad mode at 117 meV attributed to the AlO_x phonon

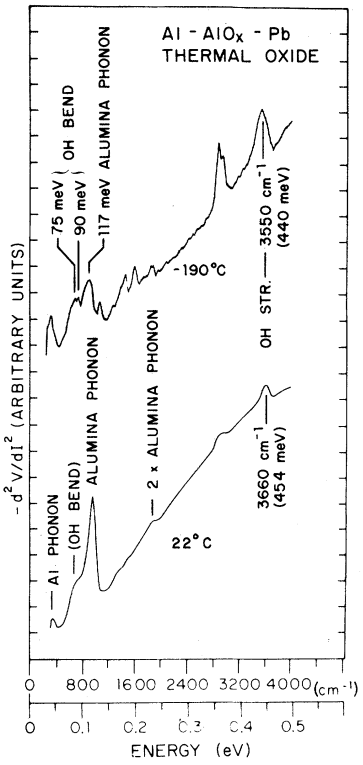

FIG. 1. Undoped Al-AlO_x-Pb junctions prepared with thermal oxide barriers; upper curve—oxide substrate cooled to −190 °C before evaporation of the Pb electrode; lower curve—Pb electrode evaporated at room temperature (22 °C). OH stretching mode is downshifted by 120 cm^{-1} when the substrate is cooled.

modes. Examples of this dominant mode are shown in the lower spectra of Figs. 1 and 3, and are recorded from junctions having barriers prepared by thermal and plasma oxidation, respectively.

Additional inelastic-mode structure is assigned to surface OH groups associated with the active sites of the aluminum-oxide barrier. These groups contribute a fairly strong OH-strectching mode normally located at ~454 meV (3660 cm^{-1}). The extreme broadness of this mode can be attributed to the existence of different active sites on the AlO_x surface and to hydrogen bonding of closely spaced surface OH groups. The OH groups also contribute bending modes at 75 and 90 meV. For barriers prepared under standard conditions, the bending modes usually appear as very weak shoulders on the lower side of the intense alumina phonon mode at 117 meV.

B. Modified AlO_x barriers

The inelastic structure contributed by the surface OH groups can be modified by using a number of different barrier-preparation procedures. One of these is the addition of excess H_2O vapor during the oxidation step. This can be done by adding H_2O directly to the vacuum system during plasma oxidation[10] or by cooling the substrate to −190 °C after thermal oxidation and before deposition of the Pb electrode. Examples are shown in Fig. 2. In either case, the OH bending and stretching modes show a strongly enhanced intensity. The OH bending modes at 75 and 90 meV become well resolved and

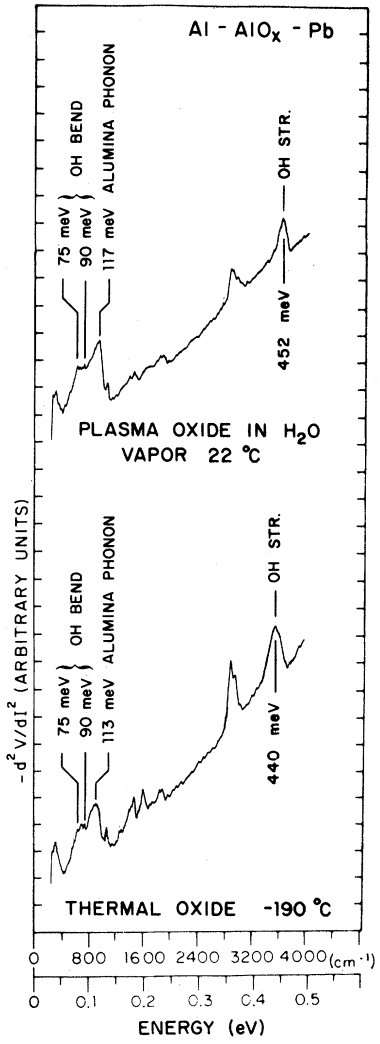

FIG. 2. Comparison of undoped junctions with barriers prepared by plasma discharge in 20 mTorr of H_2O (upper curve), and by thermal oxidation with the substrate cooled to −190 °C (lower curve). In both cases, the OH bending modes at 75 and 90 meV are enhanced.

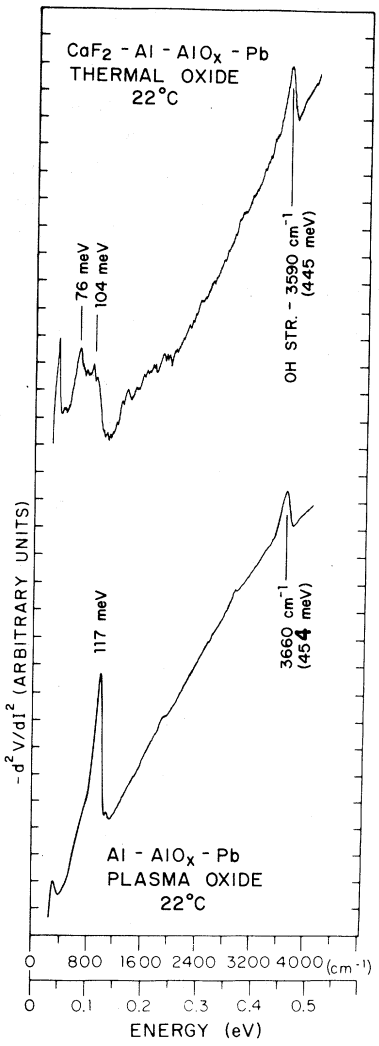

FIG. 3. OH-mode structure observed on junction prepared with a substrate roughened with an underlying CaF_2 film (upper curve). Compared to the standard plasma-discharge barrier (lower curve) prepared on a smooth substrate, the OH bending modes are enhanced and the OH stretching mode is downshifted.

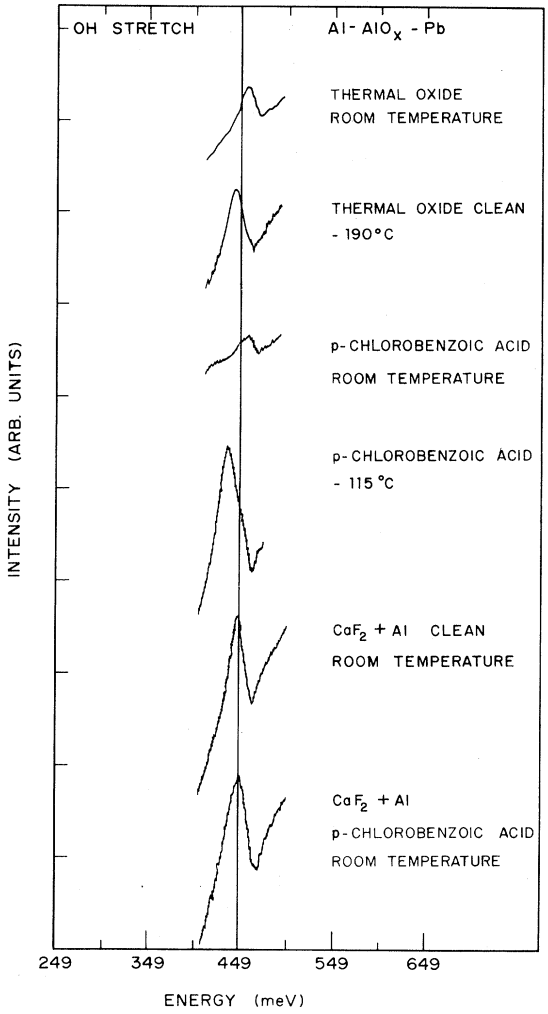

FIG. 4. Comparison of energies observed for OH stretching mode for junctions prepared under various conditions. Energy varies from 454 meV for the room-temperature thermal oxide to 438 meV for the substrate doped with *p*-chlorobenzoic acid and cooled to −115 °C.

show an integrated intensity comparable to that of the alumina phonon mode at 117 meV.

In the case of substrates cooled to −190 °C, the OH stretching mode also shows a downshift in energy of 14 meV from 454 to 440 meV. The OH mode changes induced by cooling the substrate are irreversible after evaporation of the Pb electrode. However, reheating the thermal oxide to room temperature before evaporation of the Pb electrode completely reverses the enhancement and energy downshfit of the OH-mode structure. This modification of OH vibrational modes by substrate cooling can also have a strong effect on the mode intensity of doped IETS junctions and this will be discussed in Sec. III C.

The OH enhancement produced by plasma discharge in H_2O is relatively insensitive to temperature unless the substrate is heated to above 150 °C during discharge. Bowser and Weinberg[10] showed that above 150 °C dehydroxylation of the barrier occurs and that the OH-mode structure returns to that observed for the standard barrier.

The OH-mode structure of the AlO_x barrier can also be modified by roughening the underlying aluminum electrode before preparation of the oxide barrier. This can be accomplished by first evaporat-

ing a thin film of CaF_2 on the glass substrate before evaporation of the aluminum base electrode. As the CaF_2 film is made thicker, the overlaid aluminum film has been shown to become substantially rougher.[5,6]

Subsequent thermal oxidation in air of the Al film roughened in this way produces a barrier with a large enhancement of the OH-mode structure, as shown in the upper curve of Fig. 3. The OH bending modes at 76 and 90 meV completely dominate over the alumina phonon mode intensity at 117 meV. The OH stretching mode is also enhanced and downshifted by ~ 9 meV (72 cm^{-1}). Figure 4 shows a detailed comparison of the OH-stretching-mode energies and intensities observed for the different preparation procedures. For doped junctions, this modified barrier structure produces a substantial reduction of the IETS-mode intensity, as discussed in the next section (Sec. III C). In addition, barriers produced from roughened substrates can also show time-dependent changes in the effective-barrier parameters. A model calculation is used to analyze these changes and will be discussed in Sec. IV.

C. Substrate effects on mode intensity

1. Cooled substrates

In the case of doped substrates cooled to below $-100\,°C$, the mode intensity for molecular vibrations can be substantially reduced while the OH structure is enhanced. An example of this is shown for *p*-chlorobenzoic acid in Fig. 5, which compares spectra from two junctions, one cooled to $-115\,°C$ before evaporation of the Pb electrode and the other completely fabricated at room temperature. The intensities have been compared at the same level of modulation voltage on each junction while using the same sensitivity setting on the bridge and lock-in amplifier. All of the intensity comparisons cited in this paper have been made under the above conditions.

For the cooled substrate, the broad modes associated with the OH bending vibrations below 100 meV are enhanced while the superimposed-ring-mode intensities in the same range are substantially reduced. The OH-stretching-mode intensity is also greatly enhanced as well as downshifted in energy by ~ 140 cm^{-1} (16 meV). The effect of the substrate cooling on the vibrational-mode intensity of the dopant molecule is completely reversible if the substrate is reheated before evaporation of the Pb electrode. Evaporation of the Pb electrode stops any further effects of the temperature cycling.

The degree of spectral modification induced by substrate cooling is dependent on the molecular surface coverage as well as on the type of dopant molecule. For *p*-chlorobenzoic acid the cooled substrate effect is eliminated at higher surface coverages, as measured by junction resistance. This is demonstrated for the series of spectra shown in Fig. 6, all prepared with the doped substrates cooled to $-190\,°C$. Mode reduction and enhanced OH structure are observed at low resistance, while these effects are progressively reduced as junction resistance increases. The region of enhanced OH-bending-mode intensity is indicated by the dashed lines in Fig. 6.

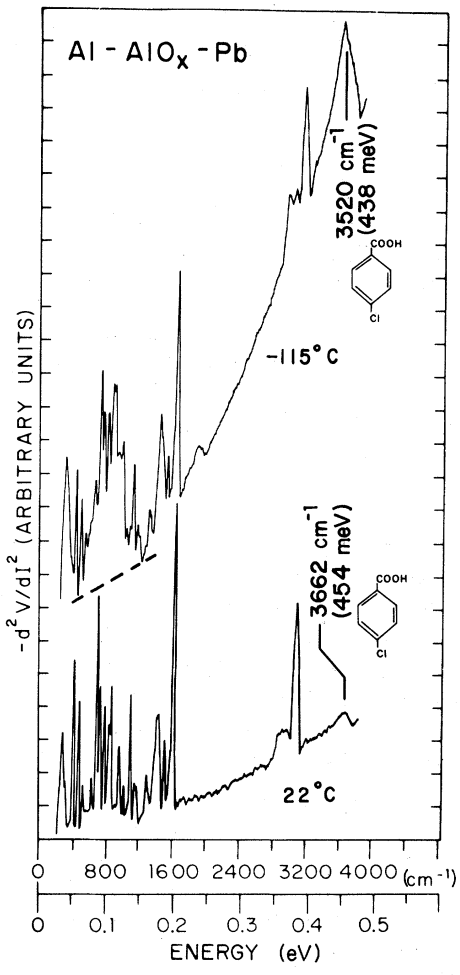

FIG. 5. IET spectra of *p*-chlorobenzoic acid obtained from Al-AlO_x-Pb junctions; lower curve—Pb electrode evaporated with substrate at 22 °C; upper curve—Pb evaporated with substrate at $-115\,°C$.

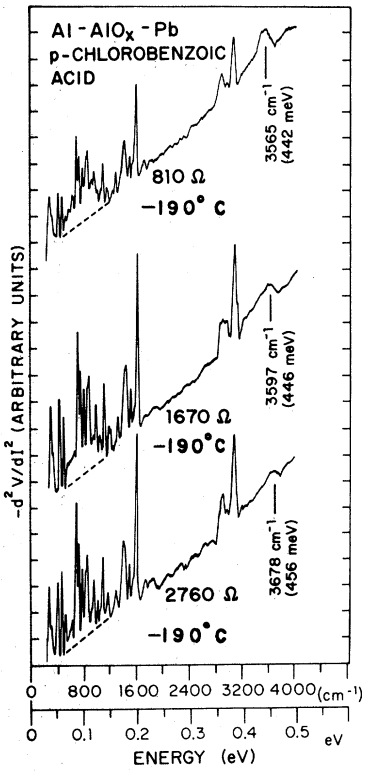

FIG. 6. IET spectra of *p*-chlorobenzoic acid obtained with substrate cooled to −190°C before evaporation of the Pb electrode. The three curves show progressively greater surface coverage corresponding to junction resistances of 810, 1670, and 2760 Ω. Enhancement of the OH bending modes (dashed lines) and the dowhshift of the OH stretching mode become progressively less at high surface coverage.

p-chlorobenzoic acid is a single aromatic ring with a COOH side group that reacts with the AlO_x surface to form a CO_2^- bidentate structure bonded to the Al^{3+} ions. The active sites of the AlO_x surface involve coordinated OH groups, and as surface coverage and junction resistance increase more and more of these sites involve an adsorbed molecule. The intensity of the IET modes has been shown to rise nonlinearly with surface concentration until a partial saturation of intensity is reached near a coverage equivalent to one monolayer.[11] Figure 7 compares the intensities as a function of junction resistance observed for junctions prepared with room-temperature substrates and with substrates cooled to −190°C. On the log-log plot of Fig. 7 the cooled substrates show a significantly greater slope, but exhibit much lower relative intensities until very high resistances are obtained. The functional relationship between surface coverage and resistance has not been established, but the data clearly confirm the strong intensity reduction induced by substrate cooling at lower coverages. Data on the strong C-C stretching mode of *p*-chlorobenzoic acid has been used for the data in Fig. 7.

2. *Rough substrates.*

A substantial reducton of IETS-mode intensity is also observed for junctions prepared on substrates roughened with CaF_2 films. The correlated enhancement of OH structure has already been outlined in Sec. III B. Figure 8 compares IET spectra obtained on rough versus smooth AlO_x substrates doped with *p*-chlorobenzoic acid. The same voltage-modulation level has been used to record both spectra giving rise to an intensity reduction by a factor of 7 for the rough substrate versus smooth.

The modifications produced in the IET spectra by substrate cooling or roughening are very similar except that the cooling is a completely reversible

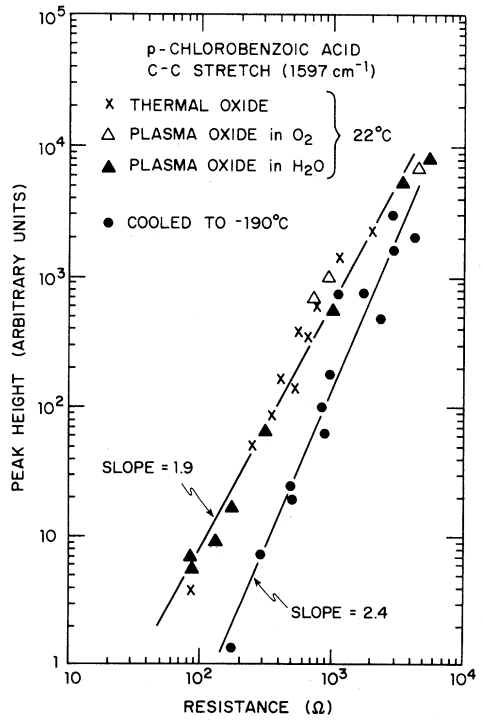

FIG. 7. Plots of peak height vs junction resistance for the C-C stretching mode of *p*-chlorobenzoic acid doped on AlO_x for substrates at 22°C and cooled to −190°C before evaporation of the Pb electrode. Data have been taken from junctions run at the same modulation voltage and bridge sensitivity or, in a few cases, the spectra have been normalized after recording.

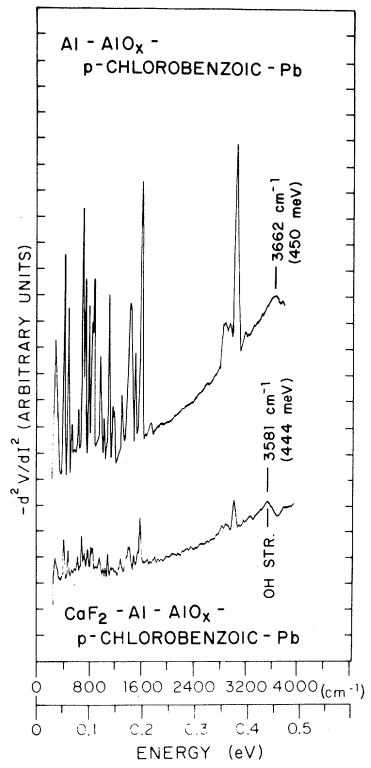

FIG. 8. IET spectra of *p*-chlorobenzoic acid obtained from doped Al-AlO_x-Pb junctions with smooth substrate (upper curve) and with rough substrate (lower curve). Substrate was roughened by first evaporating a thin film of CaF_2 before evaporation of the Al.

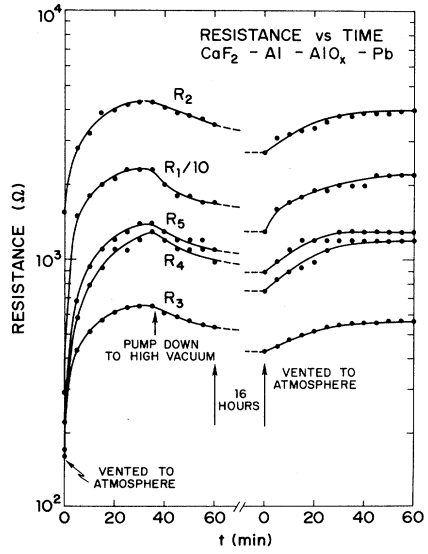

FIG. 9. Resistance of Al-AlO_x-Pb junction prepared on CaF_2 as a function of time of exposure to air and water vapor at atmospheric pressure followed by reevacuation to 10^{-6} Torr for 16 h and reexposure to room atmosphere.

process while the roughening is a permanent preparation step and the effects produced by further exposure to H_2O are only partially reversible. Both are strongly correlated with changes in the OH mode structure of the junction.

The junctions prepared with rough substrates show a time-dependent resistance change when exposed to air and water vapor, as shown in Fig. 9 for an undoped junction with a barrier prepared by thermal oxidation. An initial rapid rise in resistance is observed, a fraction of which is reversible if the junction is subsequently pumped to high vacuum again. After thermal oxidation, the experiment used to obtain the results in Fig. 9 was carried out entirely within the vacuum system and the resistances were monitored continuously.

If the rough substrate is removed and liquid doped before completion of the junction, time-dependent resistance changes are also observed upon subsequent exposure to air and water vapor. The background curvature of the d^2V/dI^2-vs-V curve also changes upon exposure to air and water vapor and shows a strong downward curvature at high bias. This is characteristic of a decreasing barrier height and is confirmed in model calculations, to be discussed in Sec. IV. In addition, the barrier calculations show that sufficient uptake of water vapor can completely reverse the initial barrier asymmetry. The resistance rise is correlated with the time-dependent changes in barrier parameters, to be discussed in Sec. IV.

IV. DISCUSSION

Water vapor is generally present in all high-vacuum systems unless very special procedures are used to eliminate it. Water adsorption on a fresh aluminum surface has been observed to lower the aluminum work function by about 1 eV.[12] This lowering is observed on both fresh aluminum or on aluminum first exposed to oxygen. The work-function results are consistent with a hydrogen outward orientation of either H_2O or OH radicals to produce a polar sheet on the initial monolayer of oxide. Further thickening of the oxide in the presence of water vapor can be expected to induce a polar structure of OH radicals that can substantially effect the electron affinity of the barrier. The main differences in the tunneling characteristics reported in the present experiments are connected with variations in the OH or H_2O structure and its effect on the barrier parameters of the tunnel junction.

A. TRAPSQR barrier

The changes in overall barrier characteristics have been monitored using a model calculation based on a trapezoidal barrier of heights Φ_1 and Φ_2 and thickness d representing the oxide, and a square barrier of height Φ_3 and thickness S representing the dopant (TRAPSQR). The barrier heights and thicknesses have been calculated by fitting the experimental I-vs-V curves to a modified WKB approximation for the tunneling current expressed as an integral of electron energy through the barrier. A least-squares computer program has been used to fit the experimental I-vs-V data over the range -1 to 1 V. The resulting barriers show systematic variations depending on the preparation treatment and type of doping molecule. The expression used for the current calculation is given in the following equation:

$$j=\frac{4\pi me}{h^3}\int_0^{E_m}\exp\left[-\frac{\sqrt{8m}}{\hbar}\int_0^{d+s}[\Phi(x,V)-E_x]^{1/2}dx\right]dE_x\int_0^{\infty}[f(E)-f(E+eV)]dE_r\ , \tag{1}$$

where m is the mass of the electron, e is the charge of the electron, $\hbar=h/2\pi$, where h is Planck's constant, x is the distance into the barrier, E is the total energy of the electron equal to E_x+E_r, E_x is the energy component in the x direction, and E_r is the component perpendicular to x. V is the bias voltage applied to the junction, $\Phi(x,V)$ is the barrier height as a function of x and V, and E_m is the maximum energy of the electron in the x direction. Further detail on the calculation as applied to the TRAPSQR barrier (model with one trapezoidal component side by side with a square one) can be found in Ref. 9. A similar model calculation has been carried out by Floyd and Walmsley.[13] In the case of undoped barriers, only the three parameters, Φ_1, Φ_2, and d have initially been used for the model calculation. However, the polarizable dipole layer due to charged-OH groups can be modeled using the TRAPSQR model and will be discussed in Sec. IV.

The barrier parameters obtained for the standard junctions prepared at room temperature without the specific addition of water vapor are listed in Table I. The thermal-oxide barrier shows a greater asymmetry than the plasma oxide, with barrier heights of 1.8 and 7.7 eV for thermal oxide, versus 2.0 and 4. 9 eV for the plasma oxide. Both types of barriers indicate an electron affinity dominated by the charged-OH structure, since the trapezoidal barriers are reversed from those expected from the work functions of the pure metals alone (Al=4.2 eV, Pb=4.0 eV). The reduction of the Al work function by H_2O and OH, as reported in Ref. 12, will contribute to such a change, but the degree of reversed asymmetry suggests a combination of reduced Al work function and specific variations of the charged-OH structure in the oxide and at the oxide-Pb interface.

B. Barrier parameter modification

In the case of undoped thermally oxidized AlO_x barriers, the asymmetry is reduced by $\sim 2-3$ eV

TABLE I. Calculated barrier parameters for room-temperature and cooled Al-AlO_x-Pb junctions.

Oxide preparation	ϕ_1 (eV)	ϕ_2 (eV)	d (Å)	$\Delta\phi$ (eV)
Smooth thermal oxide at 22 °C	1.8	7.7	10.9	5.9
Smooth thermal oxide plus H_2O at 22 °C	0.7	8.4	10.6	7.7
Smooth thermal oxide plus H_2O at -190 °C	1.8	6.7	10.5	4.9
Smooth thermal oxide plus D_2O at 22 °C	0.4	9.6	10.3	9.2
Smooth thermal oxide plus D_2O at -190 °C	0.8	7.9	10.7	7.1

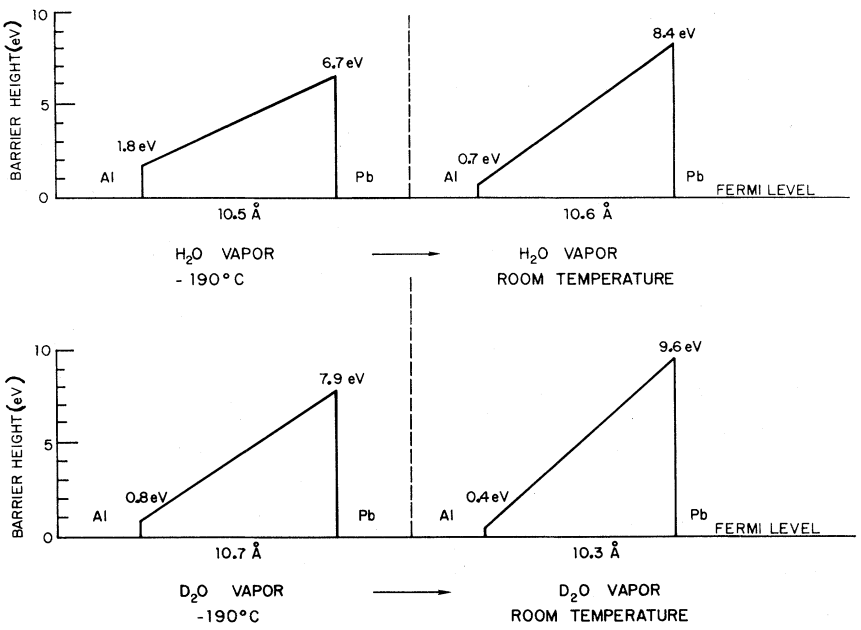

FIG. 10. Barriers of undoped Al-AlO_x-Pb junctions calculated using the TRAPSQR barrier model. Barriers were exposed to H_2O and D_2O vapor after thermal oxidation. Barriers on the left were calculated from I-vs-V curves of junctions with substrates held at -190°C during Pb evaporations. Barriers on the right were calculated from I-vs-V curves with substrates at room temperature during Pb evaporation.

upon cooling the substrate to -190°C and evaporating the Pb electrode. This effect is small within the context of the TRAPSQR model, but is reversible if the substrate is cycled back to room temperature before evaporation of the lead electrode. The relative comparison of barrier parameters for -190°C and room temperature is shown in Fig. 10 and Table I for substrates in the presence of H_2O vapor and D_2O vapor. The asymmetry is reduced by 2.8 and 2.1 eV, respectively, upon cooling the substrate to -190°C.

In the case of AlO_x barriers roughened by CaF_2 films, the effect of H_2O uptake on barrier parameters is more extreme. For undoped barriers measured immediately after removal from the vacuum system, a reduction in barrier asymmetry of several electron volts from that of smooth undoped barriers is observed but the asymmetry is still characterized by $\Phi_2 > \Phi_1$. Further exposure of the rough substrate junction to air and water vapor completely reverses the asymmetry of the barrier with $\Phi_1 > \Phi_2$. These results are listed in Table II and diagrammed in Fig. 11 for both Pb and Ag overlaid electrodes. This change of barrier asymmetry upon exposure to air and water vapor is a reversible phenomenon in that placing the junction in a vacuum system and repumping will restore the barrier asymmetry to one with $\Phi_2 > \Phi_1$.

TABLE II. Calculated barrier parameters for tunnel junctions roughened with CaF_2 and prepared at room temperature.

Junction and preparation	ϕ_1 (eV)	ϕ_2 (eV)	d (Å)
CaF_2 plus Al-AlO_x-Pb	3.6	6.0	9.7
CaF_2 plus Al-AlO_x-Pb plus air and $H_2O \sim 5$ min	6.4	3.8	10.2
CaF_2 plus Al-AlO_x-Ag	2.6	3.9	12.0
CaF_2 plus Al-AlO_x-Ag plus air and $H_2O \sim 5$ min	5.2	3.9	10.4

This reversible change in barrier asymmetry is also observed for rough barrier junctions doped with organic molecules and exposed to water vapor and air, as diagrammed in Fig. 12 for junctions doped with 5′-CMP (cytidine-5′-monophosphate). In this case, the initial oxide barrier showed an asymmetry with Φ_2 1.2 eV greater than Φ_1 and an effective organic barrier height of $\Phi_3 = 7.3$ eV. After further exposure to air and water vapor, Φ_2 was calculated to be 0.7 eV less than Φ_1 while Φ_3 was reduced to 5.0 eV. Vacuum pumpout for 12 h restored the original direction of asymmetry with Φ_2 1.8 eV greater than Φ_1 and $\Phi_3 = 6.0$ eV. The exact division between the relative barrier heights of the oxide and organic is dependent on the detailed

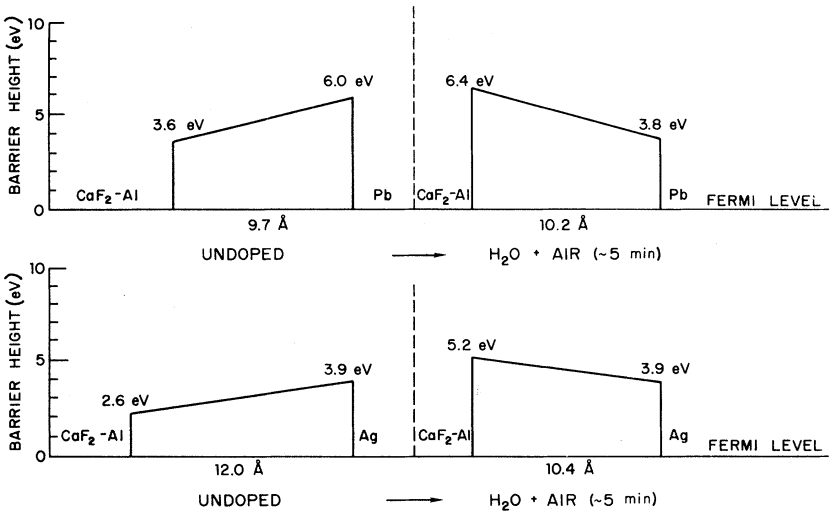

FIG. 11. Barriers calculated from I-vs-V curves obtained from Al-AlO_x-Pb junctions prepared over CaF_2 films to produce rough barriers. Barriers on left correspond to as prepared junctions. Barriers on right are calculated from I-vs-V curves obtained after exposure to air and water vapor for ~ 5 min. Upper set are for Pb electrode, lower set for Ag electrode.

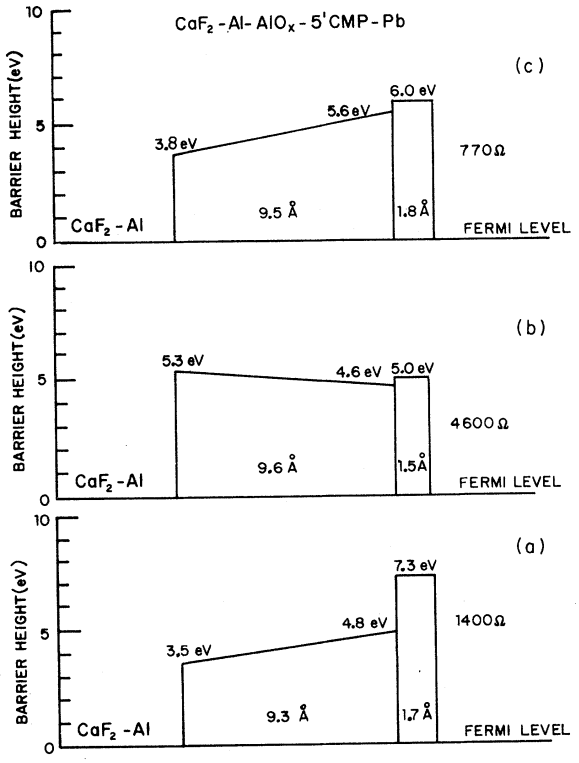

FIG. 12. Barriers calculated for Al-AlO_x-Pb junctions prepared on CaF_2 films and doped with 5'-CMP. (a) As prepared, 1400 Ω. (b) Exposed to air and water vapor for ~ 5 min, 4600 Ω. (c) Reevacuated at 10^{-6} Torr for 12 h, 770 Ω.

convergence criteria for the computer fit; however the overall changes in barrier asymmetry are clearly established and the total barrier thickness remains approximately the same for all three calculations. The calculated parameters are listed in Table III.

C. Charged OH groups

The results of both the cooled-substrate and rough-substrate experiments suggest a reversible adsorption of water vapor at the interface of the junction. This adsorption of H_2O enhances the IETS-mode intensity of both the stretching and bending modes of the OH bonds. In addition, the average OH-stretching-mode energy downshifts by up to 16 meV (130 cm^{-1}). The results suggest that, for the junction barrier, a considerable modification of the OH structure occurs for water adsorption at room temperature or below.

For pure dried γ-Al_2O_3, infrared results place the OH stretching modes in the wave-number range $3700-3800$ cm^{-1}. Peri[14] assigned the various OH configurations to five different bands within this range, the high-wave-number band at ~ 3800 cm^{-1} corresponding to an OH group with four oxide nearest neighbors in the surface and the low-wave-number band at ~ 3700 cm^{-1} to an OH group with no oxide nearest neighbors, but only four exposed five-coordinate Al^{3+} ions. The other three OH configurations were assigned to wave numbers between $3700-3800$ cm^{-1}.

TABLE III. Calculated barrier parameters for CaF_2-Al-AlO_x-(5′-CMP)-Pb junctions.

Junction preparation	ϕ_1 (eV)	ϕ_2 (eV)	ϕ_3 (eV)	d (Å)	S (Å)
Thermal oxidation at 22 °C, exposure to air ~5 min	3.5	4.8	7.3	9.3	1.7
Thermal oxidation at 22 °C exposure to air ~5 min—additional exposure to air and H_2O, ~5 min	5.3	4.6	5.0	9.6	1.5
Thermal oxidation at 22 °C, exposure to air ~5 min—additional exposure to air and H_2O, ~5 min. Repumped at 10^{-6} Torr for ~12 h	3.8	5.6	6.0	9.5	1.8

For Al-AlO_x-Pb junctions prepared under standard vacuum conditions at room temperature, the maximum of the broad OH stretching mode appears regularly near 454 meV (~3660 cm^{-1}). For alumina dried at 700 °C and then exposed to flowing wet nitrogen at 500 °C, the infrared studies show the lowest band to be a broad band just below 3680 cm^{-1} which is identified as due to closely spaced hydrogen-bonded hydroxyl groups (see Fig. 13). In the case of junctions, the overlaid lead electrode can produce a further downshift due to image effects or additional hydrogen bonding to the lead. We therefore conclude that the junction band observed with a maximum at ~3600 cm^{-1} corresponds closely to the infrared band reported above as a broad band below 3680 cm^{-1} formed when dried alumina has been reexposed to wet nitrogen.

In the case of infrared studies on alumina predried at 800 °C and then reexposed to water vapor at room temperature, corresponding to a coverage of ~40%, Peri and Hannan[15] observed that the hydroxyl band at 3795 cm^{-1} was replaced by a band near 3500 cm^{-1}. The formation of a similar band for junction barriers cooled or roughened and exposed to water vapor would account for the downshift in the OH stretching band observed in the present experiments. Peri and Hannan[15] also suggest that the broad tails below the isolated hydroxyl bands are caused by vibrations of closely spaced hydrogen-bonded hydroxyl groups which disappear when the alumina is dried.

Peri and Hannan[15] also report that undried γ-alumina aerogel shows strong, broad infrared adsorption bands near 3300 and 1650 cm^{-1} due to the stretching and deformation frequencies of molecu-

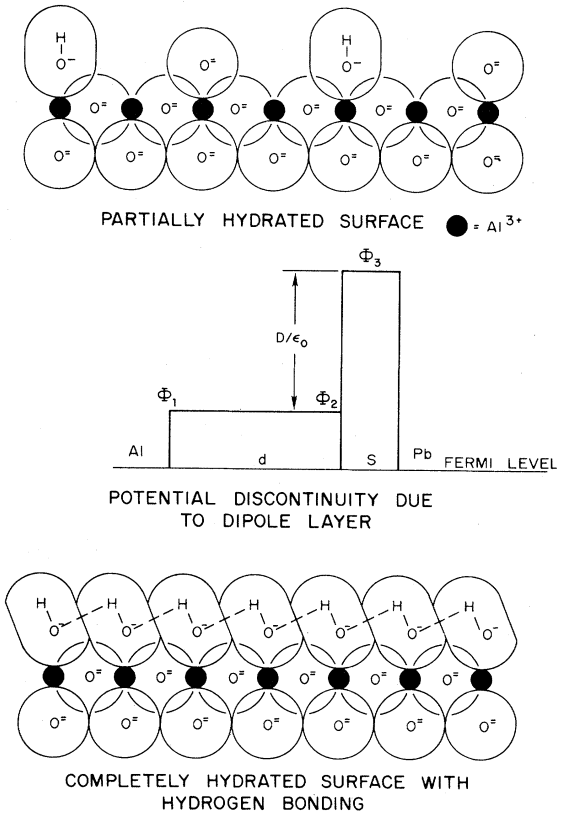

FIG. 13. Model of AlO_x barrier. Upper diagram—partially hydrated AlO_x surface, middle diagram—TRAPSQR barrier model representing oxide and polarizable dipole layer; lower diagram—completely hydrated AlO_x surface with adsorbed OH groups exhibiting hydrogen bonding.

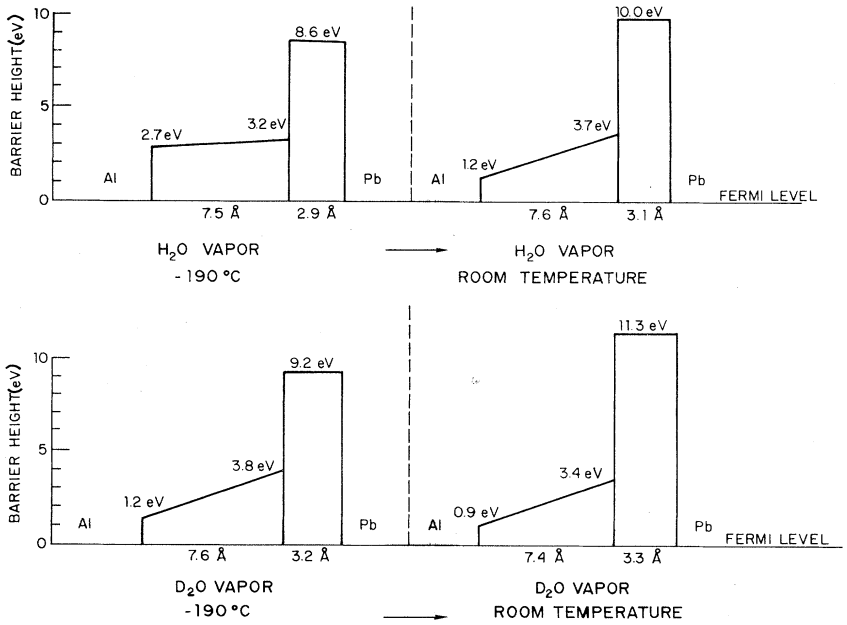

FIG. 14. TRAPSQR barrier models used to describe data from undoped junctions with dipole layers due to adsorbed OH and OD groups. Barriers describe the same data as used for the single barriers shown in Fig. 10. Reduction in asymmetry obtained by cooling the substrate is on the order of 2 eV for both models. Cooled substrate barriers are on the left and room-temperature substrate barriers are on the right.

lar water. The IETS junctions fabricated with either cooled or rough substrates do not show any substantial mode intensities at these wave numbers due to free-molecular water. As indicated in Fig. 4, a band at 3300 cm^{-1} would lie in the tail of the OH-mode intensity and a slight shoulder may be present in some cases, but the IETS intensity is dominated by the OH stretching band in all cases. The band due to the deformation vibration of molecular water at 1650 cm^{-1} is extremely close to the double-bond modes of organic molecules which all lie near 1600 cm^{-1}. However, we have not observed any substantial mode intensity for either doped or undoped junctions that could be assigned to the deformation mode of molecular water.

Hydroxyl groups involved in hydrogen bonding are favorably situated for recombination and removal from the surface as water. The tunnel junction data all point toward an increase in the density of such hydrogen-bonded hydroxyl groups due to cooling or roughening of the substrate and exposure to water vapor. A reasonable fraction of these are then easily removed by reheating or vacuum pumping.

D. Dipole-layer model

The oriented charged OH groups form a polarizable dipole layer near the oxide—Pb-electrode inter-

TABLE IV. Calculated barrier parameters for dipole model applied to Al-AlO_x-Pb junctions fabricated at room temperature and cooled to −190 °C.

Oxide preparation	ϕ_1 (eV)	ϕ_2 (eV)	ϕ_3 (eV)	d (Å)	S (Å)
Smooth thermal oxide plus H_2O at −190 °C	2.7	3.2	8.6	7.5	2.9
Smooth thermal oxide plus H_2O at 22 °C	1.2	3.7	10.0	7.6	3.1
Smooth thermal oxide plus D_2O at −190 °C	1.2	3.8	9.2	7.6	3.2
Smooth thermal oxide plus D_2O at 22 °C	0.9	3.4	11.3	7.4	3.3

face. The barrier asymmetry derived from the model calculations indicates that this charged dipole layer dominates the barrier asymmetry for most of the AlO_x barriers. The large changes in barrier asymmetry generated by the addition of water vapor can then be assigned to modifications of charge density associated with this layer.[16] The OH groups located at the different possible surface sites are calculated to have partial charges in the range $-0.5e$ to $+0.5e$. For the standard oxide barrier located between two metal electrodes, a dipole layer with dipole density D will contribute a discontinuity in potential of magnitude D/ϵ_0 as shown in Fig. 13. Assuming a surface coverage of $\sim 20\%$, an average charge of $-0.5e$ and a charge separation of 2.0 Å between the OH^- group and the Al positive ion, the value of D is calculated to be $\sim 4\times 10^{-21}$ C/Å. The discontinuity in potential would therefore be on the order of 5 V. This would contribute a positive potential barrier near the interface with the second electrode, which will in turn be terminated by the Fermi level of the second electrode.

In terms of the TRAPSQR tunneling model this will be equivalent to a high thin barrier, as shown in Fig. 14. The single trapezoidal barrier of the undoped Al-AlO_x-Pb junction can therefore be replaced by the two-barrier TRAPSQR model. The calculated parameters are listed in Table IV and are found to fit the I-vs-V data quite well with a convergence equally as good as that obtained with a single trapezoidal barrier.

The addition of water vapor and an increase in the density of surface OH groups can be expected to have two effects. The OH sites occupied at higher coverage are surrounded by more oxide molecules[14] and have a less negative charge, which should lower the vibrational frequency, as observed. Extensive hydrogen bonding on close OH groups will also further reduce the net negative charge on the OH layer. Both of these effects will lower the effective value of D and therefore lower the height of the associated barrier. This can account for the reduction of barrier height due to cooling where a reasonably flat oxide interface and associated ordered dipole layer can be expected.

The reversal of the barrier asymmetry observed for the rough barriers suggests a more complex distribution of OH groups. The roughness of the surface is estimated to be on the same order as the thickness of the barrier (20—40 Å) and therefore the geometry of the polarizable dipole regions will be more disordered. In addition, intercalation of water into the junction interface can be expected to effect the OH structure throughout most of the barrier. The model calculations again indicate a reduction in the effective dipole-layer density, but the extreme change in barrier asymmetry requires some reversal as well as reduction of the charge configuration contributing to the dipole layer.

The formation of a higher density of polarizable groups around the adsorbed dopant molecules substantially reduces the IETS-mode intensity. The IETS-mode intensity due to highly polarizable bonds such as those in an aromatic ring seem to couple strongly with the tunneling electron. Consequently, the addition of polarizable OH groups in near proximity to the adsorbed molecule might be expected to compete for interaction with the tunneling electron. As shown for the high-resistance smooth junctions doped with *p*-chlorobenzoic acid, sufficient molecular coverage can block the intensity reduction and suggests that the active sites for OH formation have been blocked if sufficient molecular coverage is obtained. The rough oxides appear to be too rough for sufficient molecular coverage to stop additional OH formation, at least at measurable tunneling resistances.

V. CONCLUSIONS

Variations in the conditions used for the preparation of aluminum-oxide tunnel barriers have been shown to have dramatic effects on the tunnel barrier heights and shapes. The variations include cooling and roughening the substrate combined with variations in the exposure to water vapor during and after fabrication. Analysis of the inelastic-electron-tunneling modes indicates that the majority of the barrier modification can be assigned to changes in the formation of charged-OH groups during and after oxidation of the aluminum electrode.

A model barrier calculation using a WKB approximation for the tunneling current and a computer-fitting procedure for obtaining a fit to the experimental I-vs-V curves has allowed quantitative comparison of the barrier parameters resulting from the different preparation procedures. In all cases the AlO_x barrier asymmetry is dominated by the charged-OH structure and the polarizable dipole layer associated with this structure. Cooling the substrate or roughening the substrate enhances the OH-mode structure and reduces the barrier asymmetry from that observed for standard room-temperature preparation of tunnel junctions using

either thermal oxidation under ambient conditions or plasma discharge in O_2. Roughening the substrate and extreme exposure to water vapor can completely reverse the barrier asymmetry.

The contribution of the OH groups can be modeled as a dipole layer which contributes a high thin barrier near the second electrode. The computer fit to a two-barrier model (TRAPSQR) fits the data for undoped junctions quite well. The changes in barrier asymmetry due to enhanced OH formation are accounted for by a reduction of the dipole-moment density and changes in the dipole configuration. An increased density of OH groups can result in a net reduction in the effective charge due to changes in the coordination to the oxide and aluminum ions and to hydrogen bonding of the close OH groups. The results of the barrier calculations and the energy shifts observed for the OH stretching vibration are all consistent with this conclusion.

The effect of enhanced OH structure on the doped junctions used for vibrational-mode analysis is generally a strong reduction in molecular vibrational-mode intensity. For smooth junctions this intensity reduction can be blocked by high surface coverage of the dopant, but for rough junctions a strong intensity reduction is observed for all useful ranges of molecular-surface coverage for IETS.

This change in IETS-mode intensity due to a variation of the detailed OH structure of the AlO_x barrier establishes a close link between the barrier structure and the quality of the IET spectrum. An initial conclusion would be that the sharp, well-defined dipole layer contributes to enhancing the IETS spectrum, possibly through the presence of a high, thin barrier as well as through the detailed polarization properties of the barrier.

These results suggest that further studies of the barrier properties and their role in IET spectra should be carried out. Barriers other than AlO_x should be more widely developed since most IETS data to date has been obtained on AlO_x barriers and the present studies show that the IET spectra are strongly correlated with the unique OH structure of this oxide. High-temperature vacuum preparation of AlO_x barriers followed by doping without exposure to water vapor would also be useful experiments.

[1]M. G. Simonsen, R. V. Coleman, and P. K. Hansma, J. Chem. Phys. 61, 3789 (1974).
[2]P. K. Hansma, Phys. Rep. 30, 146 (1977).
[3]*Inelastic Electron Tunneling Spectroscopy,* edited by T. Wolfram (Springer, New York, 1978).
[4]P. K. Hansma and R. V. Coleman, Science 184, 1369 (1974).
[5]J. G. Endriz and W. E. Spicer, Phys. Rev. B 4, 4144 (1971).
[6]H. E. Bennett, J. M. Bennett, E. J. Ashley, and R. J. Motyka, Phys. Rev. 165, 755 (1968).
[7]J. G. Adler, T. T. Chen, and J. Straus, Rev. Sci. Instrum. 42, 362 (1971).
[8]W. F. Brinkman, R. C. Dynes, and J. M. Rowell, J. Appl. Phys. 41, 1915 (1970).
[9]C. S. Korman, J. C. Lau, A. M. Johnson, and R. V. Coleman, Phys. Rev. B 19, 994 (1979).
[10]W. M. Bowser and W. H. Weinberg, Surf. Sci. 64, 377 (1977); Rev. Sci. Instrum. 47, 583 (1976).
[11]J. D. Langan and P. K. Hansma, Surf. Sci. 52, 211 (1975).
[12]E. E. Huber, Jr. and C. T. Kirk, Jr., Surf. Sci. 5, 447 (1966).
[13]R. B. Floyd and D. G. Walmsley, J. Phys. C 11, 4601 (1978).
[14]J. B. Peri, J. Phys. Chem. 69, 211 (1965).
[15]J. B. Peri and R. B. Hannan, Spectrochim. Acta 64, 1526 (1960).
[16]H. Knözinger and P. Ratnasamy, Catal. Rev. Sci. Eng. 17, 31 (1978).